Reference: *Biol. Bull.* **180:** 154–166. (February, 1991)

Distribution and Characterization of Ion Transporting and Respiratory Filaments in the Gills of *Procambarus clarkii*

JOHN S. DICKSON, RICHARD M. DILLAMAN, ROBERT D. ROER, AND DAVID B. ROYE

Center for Marine Science Research, University of North Carolina at Wilmington, 7205 Wrightsville Ave., Wilmington, North Carolina 28403

Abstract. Individual gill filaments of the freshwater crayfish *Procambarus clarkii* were determined to be either predominantly respiratory or transporting. Silver staining revealed that the filaments within the central bed of the gills formed silver deposits whereas filaments at the margins and the entire sixth pleurobranch formed no deposits. Designation of the silver staining gills as predominantly transporting and unstained filaments as predominantly respiratory was substantiated by ultrastructural analyses and measurements of ATPase and transepithelial potentials. Presumptive transporting filaments had an epithelium subjacent to the cuticle that was relatively thick and dominated by abundant mitochondria. Lacunae were delineated by pillar structures and served as collateral pathways for the movement of blood from the afferent to efferent blood channels, which were separated by a thin septum. Presumptive respiratory filaments had an extremely thin epithelium with few organelles, but a relatively thick septum. Present in both types of filaments were nerves and podocytes. The values for Na, K-ATPase were significantly higher in the transporting filaments than in those designated as respiratory. The measurement of transepithelial potentials showed both filaments to be cation selective with the respiratory filaments slightly more positive and the transporting filaments slightly more negative than the diffusion potential for Na.

Introduction

Gills are a site for exchange between the blood of the organism and the external medium and, as such, are involved in the separate but interrelated functions of gas exchange, acid/base balance, and ion regulation. Those substances exchanged may include oxygen, electrolytes, carbon dioxide, and ammonia. To produce a large surface area for such exchange, gills are often branched along one or more axes. In the crabs (Crustacea, Decapoda) lamellar gills are present (Copeland, 1963, 1968; Copeland and Fitzjarrell, 1968; Taylor and Greenaway, 1979; Finol and Croghan, 1983) and consist of a parallel afferent and efferent blood vessel between which are broad flattened sheets. In branchipod crustaceans, such *Artemia salina* and *Daphnia magna* (Copeland, 1967 and Kikuchi, 1983), amphipods and isopods (Milne and Ellis, 1973; Bubel and Jones, 1974) gills are flat, oval, sac-like extensions of thoracic appendages or modified pleopods. In crayfish and shrimp the gills are filamentous (Morse *et al.*, 1970; Bielawski, 1971; Fisher, 1972; Burggren *et al.*, 1974; Foster and Howse, 1978). In crayfish the gills are trichobranchiate and have a central stalk from which hundreds of tiny finger-like filaments arise. The podobranchia (outermost gills) are attached to the coxae of the appendages. A membranous lamina, devoid of filaments, extends from the inner side of the podobranch and lies against the thoracic body wall; its distal tip is flattened into a plate bearing a few filaments. The arthrobranchia, which are attached to the articular membrane between the body wall and the appendages, and the pleurobranchia, which are attached to the pleural wall of each somite, lie beneath the podobranchia and have no distal plate structure (Huxley, 1986; Burggren *et al.*, 1974).

Despite variations in gill anatomy, the ultrastructure of the gill epithelium in those species that are capable of osmoregulation is similar, and can be placed into one of

Received 28 June 1990; accepted 9 November 1990.

two categories. Both categories consist of a single layered epithelium that separates blood spaces from the uncalcified cuticle. One type of epithelium is relatively thick and has the characteristics of an ion transporting epithelium (see Cioffi, 1984, for a review of arthropod ion transporting epithelia). Briefly, it consists of cells with highly folded apical and basal processes, a prominent basal lamina and cytoplasm containing abundant mitochondria as well as golgi apparati, smooth and rough endoplasmic reticulum and glycogen. The second type of epithelium consists of very thin squamous cells subjacent to the cuticle. The cells are only one tenth the thickness of the previously described type, and the cytoplasm contains very few organelles (Copeland and Fitzjarrell, 1968). This ultrastructure would appear to favor diffusion of gases between the external and internal media and consequently this epithelium has been categorized as being respiratory in function.

Studies on a variety of species of decapod crustaceans have demonstrated the existence of a partitioning of ion regulatory and respiratory functions among different gills or within different regions of gills. Both morphological and biochemical (Na, K-ATPase distribution) studies have provided evidence that the anterior gills are dedicated to gas exchange while the posterior gills are involved in ion regulation in the euryhaline brachyurans *Eriocheir sinensis* (Péqueux and Gilles, 1978, 1981), *Uca pugnax* (Holliday, 1985), *Uca minax* (Wanson *et al.*, 1984), *Callinectes sapidus* (Copeland and Fitzjarrell, 1968; Neufeld *et al.*, 1980; Towle, 1984), and *Carcinus maenas* (Mantel and Landesman, 1977). Although we and other investigators realize that gill tissues possessing transport epithelia are also engaged in gas exchange, and that ions move across respiratory surfaces, we still use, for simplicity, the predominant function to designate that of the entire filament. Henceforth, we will refer to those gill filaments that possess a typical transporting epithelium as "transport" types and those gill filaments with a squamous epithelium as "respiratory" types.

Crayfish, like the euryhaline brachyurans in dilute media, exist in a hypoosmotic medium, and must maintain their ion balance by actively transporting electrolytes across the gills (Maluf, 1940; Bryan, 1959; Shaw, 1960a, b; Ehrenfeld, 1974). Unlike the euryhaline brachyurans studied, however, most crayfish are stenohaline freshwater crustaceans and possess filamentous, rather than lamellate, gills. The partitioning of respiratory and ion transporting function in the gills of crayfish is still in question. While Wheatly and Henry (1987) have used biochemical analyses of pooled gill sets to show that the distribution of Na, K-ATPase was similar among gills of *Pacifastacus leniusculus*, Morse *et al.* (1970) used silver staining and reported a partitioning of respiratory and transport functions among the gill filaments of the same species. Dunel-Erb *et al.* (1982), on the other hand, observed only respiratory epithelial tissues in the filaments and ion transporting epithelial tissues in the podobranch lamina of *Astacus pallipes* and therefore assigned the appropriate function to the two structures. The only ultrastructural observations of filaments have been of transporting epithelia (Morse *et al.*, 1970; Burggren *et al.*, 1974; Bielawski, 1971; Fisher, 1972).

This investigation was therefore directed at determining—within a single filament, within a single gill, and among gills—the distribution and frequency of the two types of epithelia of the freshwater crayfish *Procambarus clarkii*. The methods employed in this study were silver staining (Maluf, 1940), an indicator of ion transporting tissue; transmission electron microscopy (TEM), which reveals the striking difference between the morphology of the two types of epithelia; analysis for Na, K-ATPase, an effector of ion movement; and measurement of transepithelial potentials in individual filaments, which reflects possible differences in transport or permeability of the combined epithelial and cuticular layers.

Materials and Methods

The crayfish (*Procambarus clarkii*), obtained from Carolina Biological Supply, were kept in aquaria of artificial pond water (Roer and Shelton, 1982), maintained between 20°C and 25°C, and fed 2–3 times a week. Only active crayfish in the intermolt stage, as determined by the criteria of Drach and Tchernigovtzeff (1967) and Stevenson (1972), were used in this study.

Silver staining

Crayfish subjected to silver staining were first rinsed in deionized water and placed in a 0.05% $AgNO_3$ solution at 25°C for 30 min. The volume of the solution was sufficient to completely submerge the crayfish. Crayfish were then rinsed with deionized water. The branchiostegites were removed to expose the gills, and the crayfish were placed in Kodak Microdol-X developer (diluted 3:1 to lower the osmolarity to 630 mOsm) for one hour with frequent agitation. After the gills were thoroughly washed and placed in distilled water, one or two drops of NH_4S were added to intensify the stain.

Preparation of gill filament tissues for electron microscopy

Silver treated filaments were fixed in 3% glutaraldehyde in 0.1 *M* cacodylate buffer (pH 7.2) containing 5% sucrose (osmolarity = 640 mOsm) at 25°C for at least 1 h. To facilitate penetration of the various solutions, the tips were cut off the filaments and the tissue was gently agitated at each step of the preparation. The filaments were then

rinsed in buffer and postfixed with 2% osmium tetroxide in 0.1 *M* cacodylate buffer (pH 7.2) plus 5% sucrose at 25°C for 2 h. After another rinse with buffer, tissues were dehydrated with a graded series of ethanol and propylene oxide, and embedded in Spurr low viscosity embedding medium (Spurr, 1969).

Filaments not silver-treated were fixed in 2% glutaraldehyde in 0.15 *M* cacodylate buffer, pH 7.4, with 5 m*M* $CaCl_2$ for 1 h, rinsed in buffer, and post-fixed in fresh 0.5% OsO_4 with 0.8% $K_4Fe(CN)_6$ in 0.1 *M* cacodylate buffer, pH 7.4, with 5 m*M* $CaCl_2$ at 25°C for 1 h. After rinsing again in cacodylate buffer, the tissues were placed in 0.15% tannic acid in 0.15 *M* cacodylate buffer, pH 7.4, with 5 m*M* $CaCl_2$ for 5 min. Following a short rinse in buffer and distilled water, the tissues were stained *en bloc* with 2% aqueous uranyl acetate for 2 h. After a distilled water rinse, tissues were dehydrated through a graded series of acetone and embedded in Spurr.

Cross-sections were cut in the basal, medial, and distal regions of the filaments. Sections were post-stained with 4% uranyl acetate in 50% ethanol and Reynolds lead citrate (Reynolds, 1963), and were viewed with a Zeiss EM 9S transmission electron microscope operated at 60 kV.

Na, K-ATPase assay of filaments

Na, K-ATPase assays were done according to the method of Horiuchi (1977). After washing excised gills in 0.25 *M* sucrose buffered to pH 7.5 with 100 m*M* Tris-HCl, predicted transporting or respiratory filaments were removed from the gills, pooled by type, and homogenized at 4°C in 2 volumes of the buffered sucrose solution during 35 passes in a glass tissue homogenizer. The homogenate was centrifuged at 3000 × *g* for 15 min and the supernatant was assayed for activity.

The reaction mixture consisted of 60 m*M* NaCl, 20 m*M* KCl, 2 m*M* $MgCl_2$ and 30 m*M* Tris-HCl, pH 7.5, in 0.8 ml. This reaction mixture was preincubated at 32°C before 0.1 ml of the enzyme solution and 0.1 ml of the 3.0 m*M* Tris-ATP were added. The enzymatic reaction was allowed to proceed for 45 min, being terminated by the addition of cold 3% trichloroacetic acid. The amount of inorganic phosphate, hydrolyzed from ATP, present in the supernatant was measured according to Wheeler (1975). Mg-ATPase activity was determined as above with the substitution of 10 m*M* ouabain for KCl in the reaction mixture to inhibit Na, K-ATPase. Na, K-ATPase activity was calculated as the difference between the total ATPase and Mg-ATPase values. The amount of protein was determined according to Peterson's (1977) modified Lowry protein assay using a Bausch and Lomb Spectronic 710 spectrophotometer and bovine serum albumin as a standard. The specific activities were recorded as micromoles of inorganic phosphate per milligram of protein per hour.

Transepithelial potential measurements

Crayfish were submerged in ¼ strength Van Harreveld's Ringer solution (final concentrations: NaCl = 51.3 m*M*; KCl = 1.3 m*M*; $CaCl_2$ = 3.4 m*M*; $MgCl_2$ = 0.3 m*M*) in a finger bowl, and restrained by rubber bands attached to a notched plexiglass plate. Diluted Ringer's solution was used to provide sufficient electrolytes for electrode conduction. Potentials measured with pond water as the external medium were unreliable. The branchial region of the carapace was cut away from one side of the animal to expose the gills. In this position, individual gill filaments could easily be impaled by glass microelectrodes using a micromanipulator.

Microelectrodes were drawn from glass capillary tubing and filled with 3 *M* KCl. A Ag-AgCl reference electrode was immersed in the bathing medium. Both electrodes were connected by shielded cables to a WPI model 701 microprobe system and a Tectronix 5111 storage oscilloscope.

Only filaments of the podobranchs were impaled and the assignment of putative transport and respiratory filaments was based upon the results of the silver staining experiments. Transepithelial potentials (TEP's) and the position of the electrode tip within the filament were recorded each time a gill was impaled. Sodium concentrations of the medium and crayfish hemolymph were measured by flame photometry (Turner model 510).

Results

Silver staining

In six crayfish subjected to silver staining all showed some staining in all gills except pleurobranch 6. Staining occurred only in the filaments. That is, no staining was observed in the central gill stalk, in the lamina, in the distal plate of the podobranchia, nor at the base of the gills. Figure 1 is representative of the filament staining patterns. The podobranchs had the largest proportion of stained filaments, whereas the pleurobranchs had the least for each set of gills. All gills showed the same basic pattern, a population of stained filaments in the central area of the filament bed surrounded by lateral rows of unstained filaments, with the exception of the pleurobranch of the sixth gill set, which showed no silver staining. Silver stained filaments had precipitate distributed evenly over the length of the filament.

Transmission electron microscopy of silver stained filaments showed that most of the precipitate was within the gill cuticle, although lesser amounts were observed outside or beneath the cuticle (Fig. 2). Precipitate within the cuticle was localized almost exclusively in a layer corresponding to the exocuticle, rarely being found in the epicuticle or endocuticle. While the treatment employed

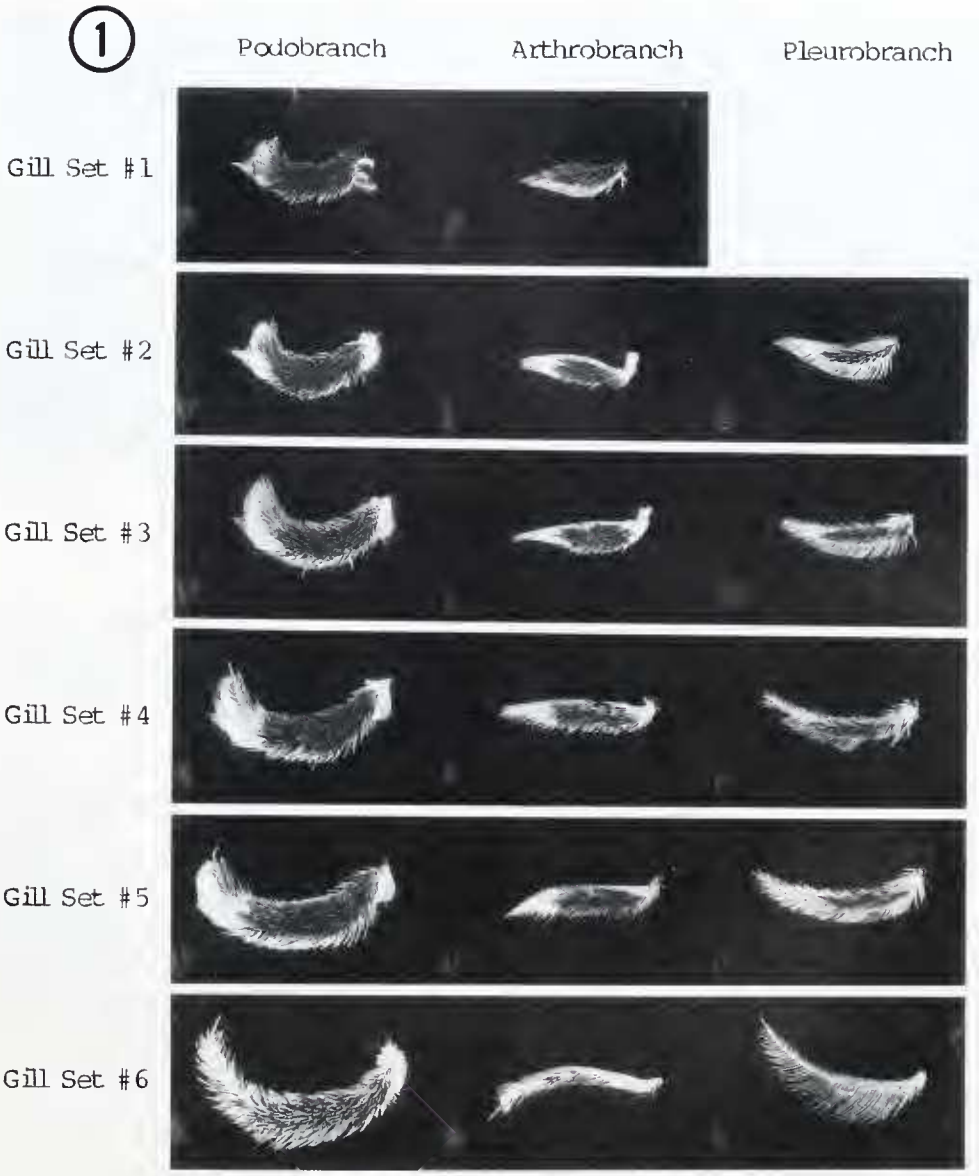

Figure 1. Light micrographs of six sets of gills from the right side of a crayfish after silver staining. Each gill is oriented with the base to the right. Dark staining indicates silver deposition.

in the silver staining disrupted the soft tissues, it was possible to note that the epithelium underlying the cuticle was relatively thick and had numerous basal and apical infoldings. Filaments containing no precipitate after silver treatment (Fig. 3) had an epithelium subjacent to the cuticle that was markedly thinner than that of the silver stained filaments and had few, if any, basal and apical infoldings.

Ultrastructure of the gill filaments

Choice of filaments for ultrastructural analysis of presumptive ion-transporting and respiratory tissue was based upon the distribution of the two types as indicated by silver staining (Fig. 1) and proved to be accurate in all 20 of the filaments examined. No differences were observed among sections from proximal, medial, or distal regions of a filament. Diagrammatic representations of cross sections through the two types of filaments are seen in Figures 4 and 5. The transporting filaments, regardless of the gill set, had a diameter of 0.1 mm to 0.2 mm, while the respiratory filaments were 0.2 mm to 0.3 mm in diameter. Both types of filaments contained an afferent and an efferent blood channel and lateral lacunae. The afferent channel was on the side of the filament that faced toward the gill stalk, and the efferent channel on the side that

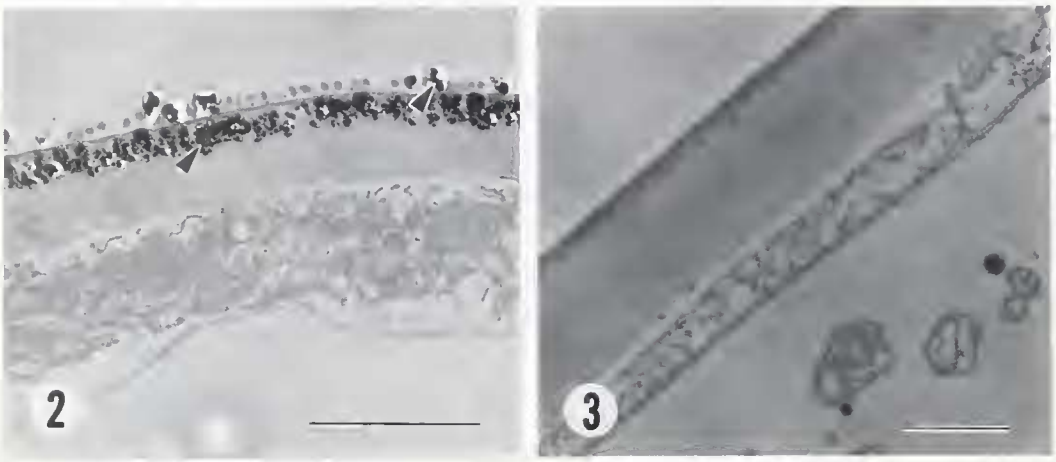

Figure 2. TEM of transporting gill filament after silver staining. Note crystals within and on the cuticle (arrows). Bar = 5 μm.

Figure 3. TEM of respiratory gill filament after silver staining. Bar = 1.0 μm.

faced away from the stalk. A septum and the surrounding connective tissue separated the two major blood spaces. An epithelium, 80–90% of which occurred in the lacunar blood space, lined the noncalcified cuticle of the filaments. Epithelial cells extended across the lacunae forming pillar structures with their basal portion embedded in loose connective tissue. Also depicted is the marked difference in epithelial thickness within and between the filament types.

In the transporting filaments, the cuticle epithelium bordering the afferent channel was the thickest (approximately 6 μm) (Fig. 4). Numerous mitochondria, generally oriented perpendicular to the cuticle, were observed and were most abundant in the apical portion of the cells (Figs. 6, 7, 8). Apical microvillar processes were approximately 80 nm wide and varied in length from 0.4 μm to 1.2 μm (Fig. 8). Electron-dense material was observed between the tips of the microvilli and the overlying cuticle (Fig. 9). Numerous infoldings and interdigitations occurred in the basal region of the epithelium (Figs. 6, 7). The microtubules observed within the cytoplasm were oriented nearly perpendicular to the cuticle and were often closely apposed to mitochondria (Fig. 8). Occasional golgi apparati were observed in the epithelium lining the outer margin of the afferent canal (Fig. 6), as well as a thin basal lamina (Figs. 6, 9). Adhering junctions occurred apically on lateral cell membranes, below which were septate junctions. Gap junctions were observed below the septate junctions (Fig. 6).

The portion of the epithelium lateral to the septum and on the efferent side of the filament was thinner (approximately 1.5 μm) than that portion bordering the afferent canal, but also contained numerous mitochondria and microvillar processes (Fig. 9).

The epithelial cells forming the pillar structures had a highly convoluted basal nucleus (Fig. 7) and were usually rich in mitochondria, rough endoplasmic reticulum, and golgi apparati (Fig. 8).

The cuticle of the transporting gill filaments was of uniform thickness (approximately 1.8 μm) around their entire circumference. An outer thin epicuticle, the thin lamellae of the exocuticle, and the thicker lamellae of the endocuticle were easily differentiated in most sections (Figs. 6, 9). The approximate thicknesses of the exocuticle and the endocuticle were 0.8 μm and 0.6 μm, respectively.

The septum traversed the central blood space, joining the loose connective tissue on either side of the filament, thereby forming a partition between the afferent and efferent blood channels (Figs. 4, 5, 10, 16). Along the efferent channel the septum was relatively smooth, whereas the side facing the afferent channel possessed processes that extended into the channel (Figs. 10, 16). In the transporting filaments the septum was relatively thin (approximately 1.1 μm) (Fig. 10) and became shorter as the filament tapered in its distal portions. Numerous membranes were observed along the length of the septum, some of which constituted the cell membranes of loose connective tissue cells on either side of the filament. A thin basal lamina was observed on the efferent side of the septum, and a thicker fibrous basement membrane covered the afferent septal process (Figs. 10, 16).

The epithelium of the respiratory filament varied in thickness, ranging from 0.7 μm opposite the septum to 3.0 μm in regions adjacent to pillar structures (Figs. 5, 11). A few scattered round or oval mitochondria were observed in the granular cytoplasm whereas thicker regions of the epithelium adjacent to the pillar cells also had some glycogen granules (Figs. 12, 13). The regions of

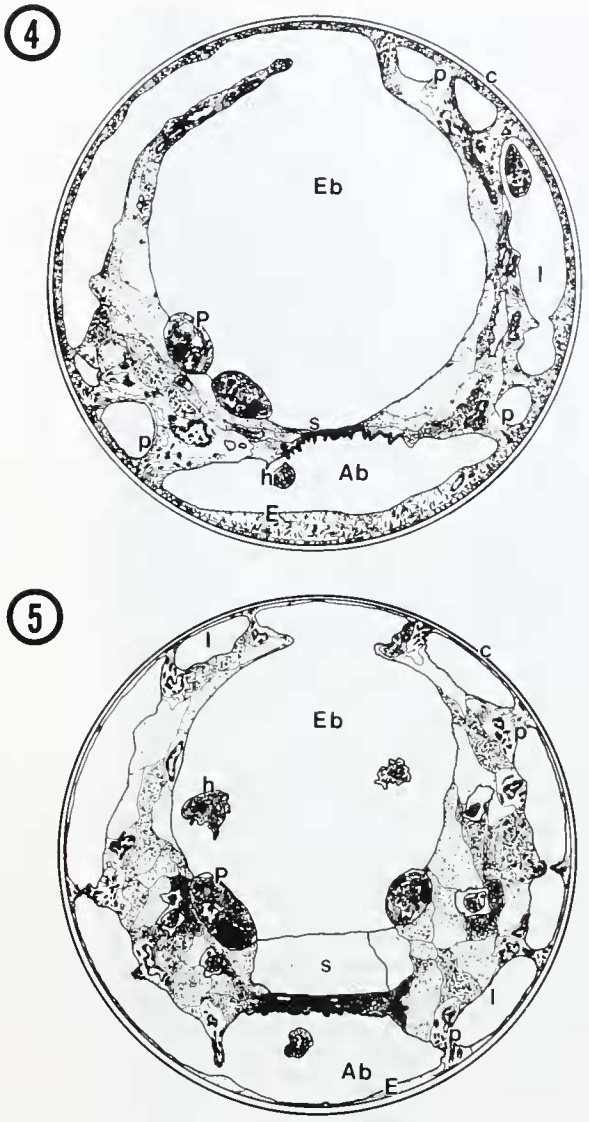

Figures 4 and 5. Diagrammatic representations of cross sections through a transporting (Fig. 4) and respiratory (Fig. 5) gill filament. Note the afferent blood channel (Ab), efferent blood channel (Eb), epithelium (E), cuticle (c), septum (s), podocyte (P), hemocyte (h), pillar structure (p), and lacuna (l).

the epithelium lateral to the septum and on the efferent side of the filament were much thinner, having a width as small as 0.08 μm (Figs. 11, 14). The epithelium was lined by a thin basal lamina and had a sparse cytoplasm containing microtubules. Fibrous material was also seen between the basal lamina and the epithelium. No apical microvillar processes or basal infoldings were observed in the respiratory filament epithelia.

The most prominent feature of the cells in the pillar regions was the bundles of microtubules observed in their cytoplasm (Figs. 12, 13). These bundles were generally oriented perpendicular to the cuticle, apparently attached to extensions of the cuticle that penetrated into the epithelial cells (Fig. 13). The pillar cytoplasm contained some mitochondria, rough endoplasmic reticulum, and golgi, but noticeably fewer than in the transporting filament tissues (Fig. 12).

The cuticle of the respiratory filaments was thickest on the side of the afferent channel (approximately 2.0 μm) (Fig. 14) and thinnest on the efferent side of the filament (approximately 0.5 μm) (Fig. 15). The attenuation of the cuticle from the afferent to the efferent side was observed lateral to the septum of the filament. It appeared as if no endocuticle had been deposited on the afferent side of the filament, the side facing the carapace.

The septum of the respiratory filament was thicker than the transporting filament septum, possessing afferent septal projections, a thick afferent basement membrane, and a thin efferent basal lamina. The septum had a width of about 5 μm, with an abundance of cell membrane interdigitations (Figs. 5, 16). A thick layer of fibrous material frequently lined the inside of the cell membrane on the afferent side of the septum (Fig. 16). Thicker septa observed in these filaments usually had loose connective tissue extending across the septum on the afferent side (Fig. 5).

Neural tissue was often observed in both filament types (Fig. 17). The small nerves were located within one of the small blood spaces of the connective tissue lateral to the septum. Usually there was one nerve per filament, though a few filaments were observed that contained two or three nerves, each in a separate blood space. The nerve was continuous throughout the length of a filament. Nerves ranged from 1.0 μm to 2.7 μm in diameter and contained two to six neurons. The neurons, which ranged from 0.16 μm to 1.5 μm in diameter, contained numerous, evenly spaced neurotubules. No cell bodies, neurosecretory granules, or synapses were observed in any section.

Also occurring in both types of filaments were cells resembling "podocytes" (Morse *et al.*, 1970). They were observed near the septum, attached to the loose connective tissue bordering the afferent channel (Figs. 4, 5, 18) and were surrounded by a basal lamina. These cells possessed an interdigitating cell membrane, or pedicels, which formed extracellular spaces between the pedicels and the cell body. Much of the cytoplasm contained an abundance of smooth endoplasmic reticulum. Coated pits and vesicles were often observed along or near the cell membrane and numerous dense granules, varying in size and number, occurred within the cytoplasm along with golgi apparati consisting of thin, curved cisternae (Fig. 19).

ATPase determinations

As shown in Figure 20, the mean for total ATPase activity was higher in the transporting than in the respiratory

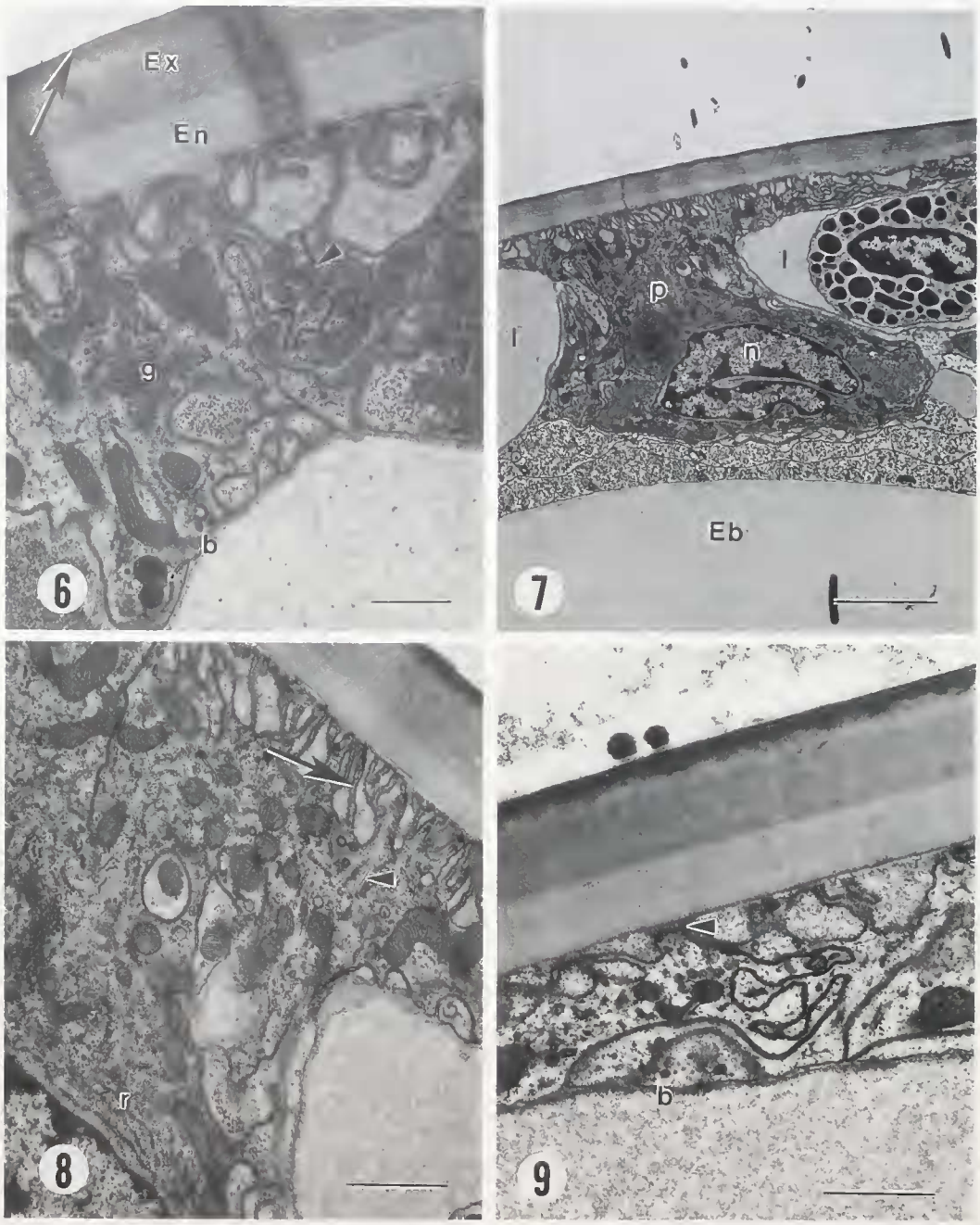

Figures 6–9. TEM of transporting filaments. **Figure 6.** Section showing the cuticle with its three layers, the epicuticle (arrow), the exocuticle (Ex) and the endocuticle (En). Also note a Golgi apparatus (g), the basal lamina (b), and a junctional complex (arrowhead). Bar = 1.0 μm. **Figure 7.** Section showing a pillar structure (p) separating two lacunar spaces (l) from an efferent blood channel (Eb). Note heterochromatic nucleus (n). Bar = 5.0 μm. **Figure 8.** Section of epithelium under cuticle showing microtubules (arrowheads) and rough endoplasmic reticulum (r) in the cytoplasm. Also note the apical microvillar structures (arrow) immediately below the cuticle. Bar = 1.0 μm. **Figure 9.** Section of epithelium between cuticle and lacuna showing the electron dense material at the tip of the microvillar processes (arrowhead) and the thin basal lamina (b). Bar = 1.0 μm.

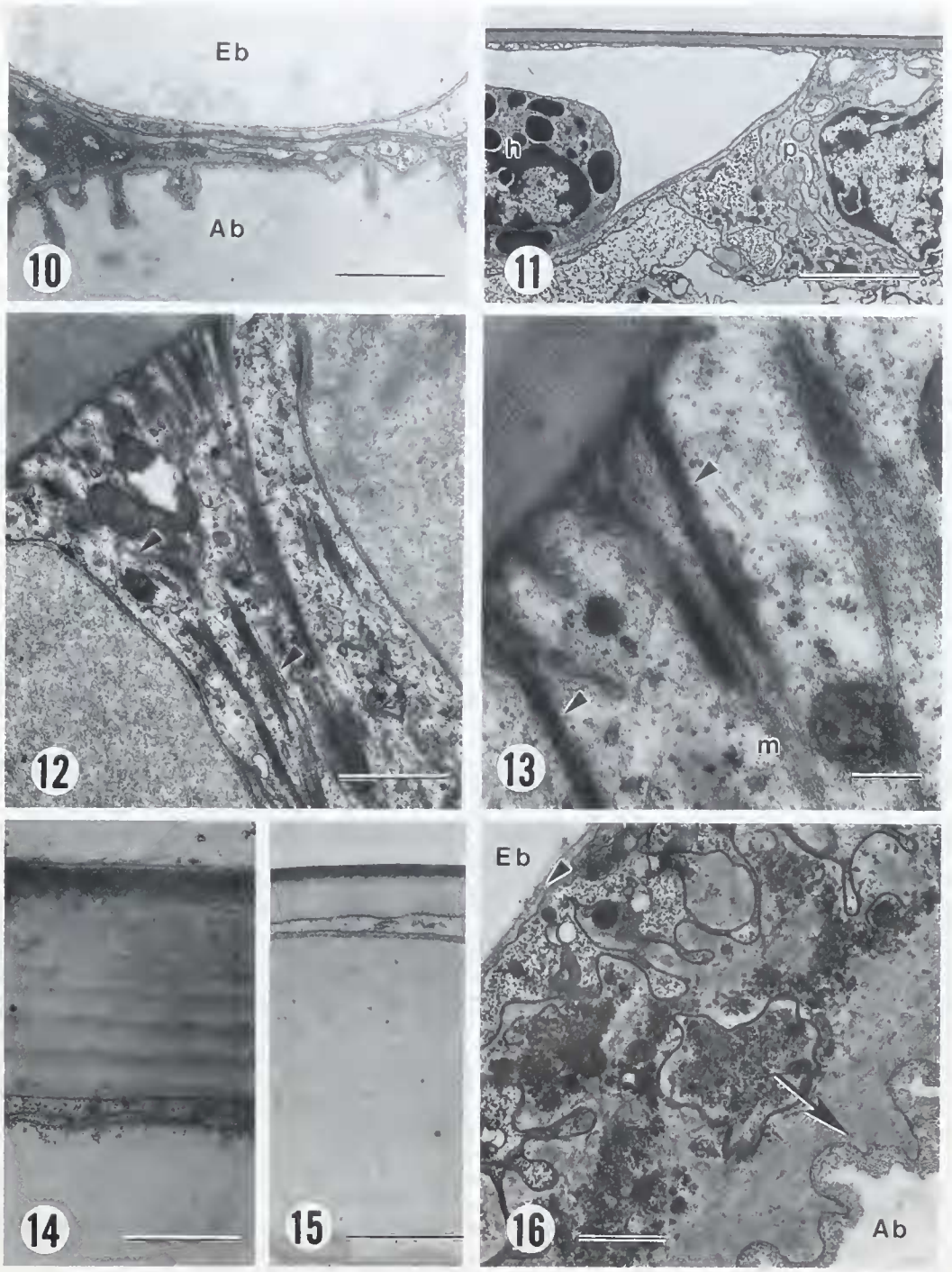

Figures 10–16. TEM of transporting (10) and respiratory (11–16) filaments. **Figure 10.** Section of a septum in a transporting filament that separates the afferent (Ab) from the efferent (Eb) blood channel. Bar = 2.0 μm. **Figure 11.** Section of a respiratory filament showing the thin epithelium underlying the cuticle. Also note the pillar structure (p) and a hemocyte (h). Bar = 5.0 μm. **Figure 12.** Pillar structure of a respiratory filament showing the bundles of microtubules running perpendicular to the cuticle (arrowheads). Bar = 1.0 μm. **Figure 13.** Section showing relationship of microtubules (m) to extensions of the cuticle (arrowheads). Bar = 0.2 μm. **Figure 14.** Cuticle on side of afferent channel. Bar = 1.0 μm. **Figure 15.** Cuticle on side of efferent channel. Bar = 1.0 μm. **Figure 16.** Septum from respiratory filament separating the afferent blood channel (Ab) from the efferent blood channel (Eb). Note the thin basal lamina on the efferent side (arrowhead) as compared with the thick layer on the afferent side (arrow). Bar = 1.0 μm.

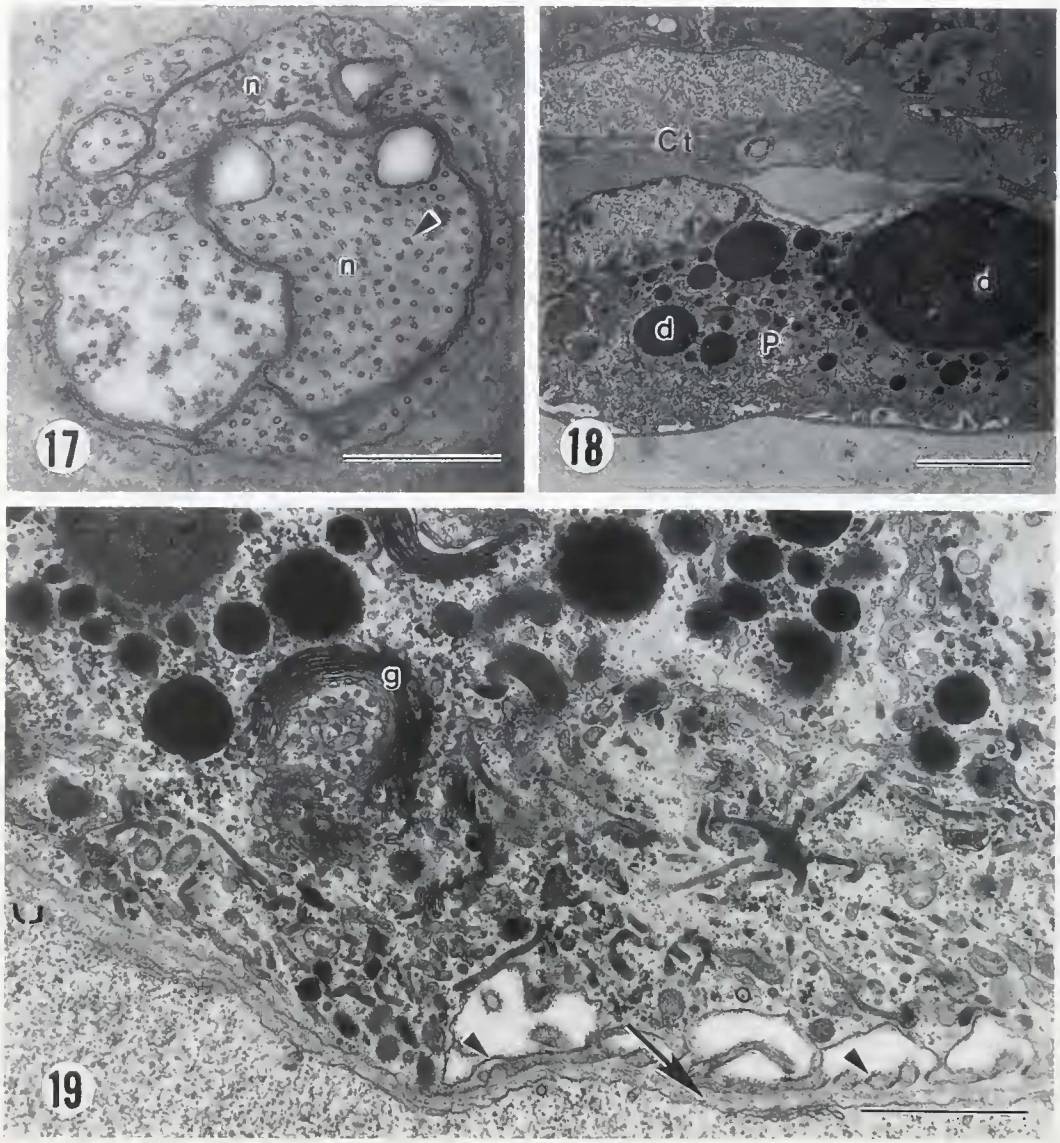

Figures 17–19. TEM of filaments. **Figure 17.** Cross section of nerve showing individual neurons (n) having evenly spaced neurotubules (arrowheads). Bar = 0.5 μm. **Figure 18.** Podocyte (P) in loose connective tissue (Ct). Note electron-dense inclusions (d). Bar = 5.0 μm. **Figure 19.** Podocyte cytoplasm showing pedicels (arrowheads) golgi (g) and basal lamina (arrow). Bar = 1.0 μm.

filaments; however, the difference between the means was not significant. Mean values for Mg-ATPase were very similar between respiratory and transporting filaments and were likewise not significantly different. The means for Na, K-ATPase, in contrast, were significantly different ($P < 0.001$, Mann-Whitney U test), with the transporting filaments having more than five times as much mean activity as the respiratory filaments.

Transepithelial potentials

The values of the TEP's in the filaments were independent of the region (proximal, medial, or distal) of the filament impaled and of the podobranch upon which the filament was located. The TEP's of filaments that were presumed to be respiratory (based upon the silver staining results) ranged from −6 to −18 mV (−11.9 ± 3.2 mV, mean ± S.D., n = 19). The TEP's measured in presumptive transport filaments ranged from −21 to −36 mV (−28.1 ± 4.7 mV, mean ± S.D.; n = 21). There was no overlap in the frequency distributions of the ranges of TEP's (Fig. 21) and the difference between the means was highly significant ($P < 0.001$, two-tailed t test). The sodium concentration of the medium was 51 mM and that of the hemolymph was 107.5 ± 15.0 mM (mean ± S.D., n = 11).

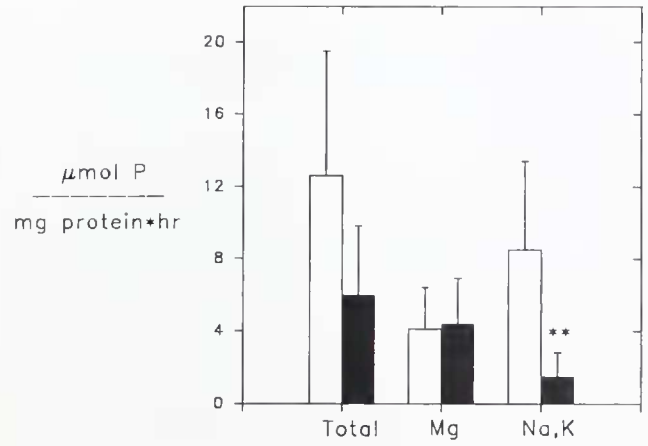

Figure 20. Mean (± standard deviation) ATPase activity comparing pooled transporting (open bars) and respiratory (solid bars) filaments. ** = $P < 0.001$

Discussion

The results of silver staining, ultrastructural analyses, ATPase measurements, and measurements of TEP all indicate that the gills of *P. clarkii* are not homogeneous in structure, but contain filaments dedicated to ion transport and filaments dedicated to respiration. No filaments had both characteristics; rather individual filaments were uniquely respiratory or transporting. Respiratory filaments occurred on the lateral rows of most gills, whereas the transporting filaments predominated in the central bed of the gills. This distribution of the two filament types in discrete regions of the gill placed the respiratory filaments in the path of the most rapid water flow (Burggren *et al.*, 1974).

The respiratory filaments had a very thin, squamous epithelium, whereas the ion transporting filaments possessed a markedly thicker epithelium. The ultrastructure of the ion transporting epithelia observed in *P. clarkii* gill filaments was similar to ion transporting epithelia described in other crayfish (Morse *et al.*, 1970; Bielawski, 1971; Fisher, 1972), in isopods (Bubel and Jones, 1974), in crabs (Copeland and Fitzjarrell, 1968; Taylor and Greenaway, 1979; Finol and Croghan, 1983), in shrimp (Foster and Howse, 1978), and in *Daphnia* (Kikuchi, 1983). Apical microvillar processes were present to increase the surface area over which ions could be transported as well as numerous basal infoldings with associated mitochondria. Such basal infoldings are reported to be the major site of Na, K-ATPase (Diamond and Bossert, 1968; Ernst, 1972; Ernst *et al.*, 1981; Towle, 1985; Towle and Kays, 1986). This would be consistent with the higher Na, K-ATPase activity measured in transporting filaments, because few basal infoldings or mitochondria were observed in the epithelia of the respiratory filaments.

The structure of the thin squamous epithelia in *P. clarkii* respiratory filaments was similar to the respiratory epithelia described in other crayfish (Dunel-Erb *et al.*, 1982) in crabs (Copeland and Fitzjarrell, 1968; Taylor and Greenaway, 1979), and in shrimp (Foster and Howse, 1978). The paucity of organelles observed in the epithelium and pillar structures indicates that little cellular activity occurs in these cells other than maintenance of cell components. The thin epithelial layer may serve as a permeability barrier to the diffusive loss of ions and blood proteins, while the thin cytoplasm would allow efficient gas exchange to occur.

Large bundles of microtubules were observed in the pillar structures of the respiratory filaments, whereas single microtubules were the rule in the transporting epithelia of this crayfish and in most gill epithelia of other crustaceans (Copeland and Fitzjarrell, 1968; Bielawski, 1971; Foster and Howse, 1978; Taylor and Greenaway, 1979; Finol and Croghan, 1983; Compère *et al.*, 1989). These microtubules appear to anchor the epithelium to the cuticle. Finol and Croghan (1983) have proposed that the microtubules function to stabilize the gill epithelium against the hydrostatic pressure of the blood. Because the respiratory epithelium contains very little cytoplasm, additional microtubules, in the form of bundles near the periphery of the pillar structures, may give the additional support needed to withstand the shear forces of the blood flow in these filaments.

The loose connective tissue in the gills of *P. clarkii* is similar to that observed in *Callinectes sapidus* (Johnson, 1980). The cells within the loose connective tissue, with their abundant glycogen rosettes and granules, may regulate the blood glucose levels as suggested by Finol and Croghan (1983) for *Uca morda*.

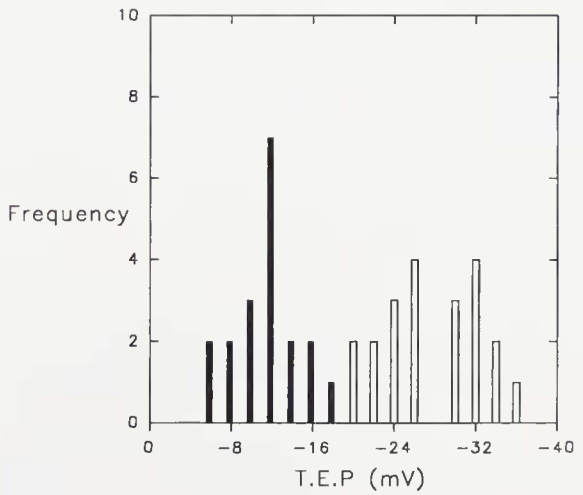

Figure 21. Transepithelial potentials (TEP) for respiratory (solid bars, n = 19) and transporting (open bars, n = 21) filaments.

The observed difference in the size and structure of the septum in the two types of filaments suggests its function may likewise differ. The thicker septum in the respiratory filaments may make the vascular canals more rigid, or it may also be a more substantial barrier to diffusion between the two compartments.

The neurons observed in the filaments of *P. clarkii* were similar to those constituting the branchial nerve observed in *A. pallipes* and *A. leptodactylus* (Dunel-Erb *et al.*, 1982). While those authors have described the nerve cell bodies and described structures resembling neurosecretory granules, the role of the nerve is uncertain. Massabuau *et al.* (1980) and Ishii *et al.* (1989) have suggested that the nerve may serve peripheral sensory elements involved in oxygen sensing. While the presence of the nerve in both the respiratory and transporting filaments would seem to question this function, the absence of any description of a transducing element leaves this question unresolved.

The "podocytes" observed in the filament tissues possessed the same ultrastructure as "podocytes" observed in other crustacean gills (Wright, 1964; Strangeways-Dixon and Smith, 1970; Doughtie and Rao, 1981). The presence of coated vesicles and large storage vacuoles gives support to the hypothesis that these cells take up toxic substances and blood components from the hemolymph for degradation or storage (Strangeways-Dixon and Smith, 1970; Doughtie and Rao, 1981).

ATPase measurements supported the silver staining and morphological observations in that values were highest in the transporting filaments. These data represent an apparent contradiction to the conclusion of Wheatly and Henry (1987) who reported that enzyme activity was homogeneously distributed throughout the branchial tissue. However, Wheatly and Henry (1987) pooled tissue from entire gill sets, and, therefore, could not have detected differences at the level of individual filaments. In fact, their data would represent a mean of respiratory and transporting filaments, assuming that *Pacifastacus* has a distribution of filament types similar to *Procambarus*. Our values for Na, K-ATPase activity in respiratory filaments are comparable to theirs, but the values we obtained for transport filaments are fivefold higher, reflecting the enrichment of transport tissue resulting from analyses of selected filaments.

While the *in situ* measurements of TEP's in the gill filaments were not intended to supply extensive data on the mechanisms of transport, a few interesting conclusions may be made. The data clearly suggest two functionally different populations of filaments. These data are qualitatively similar to those of Péqueux and Gilles (1988) who found positive TEP's in isolated, anterior, respiratory gills of *Eriocheir*, but negative potentials in the posterior, transporting gills.

The fact that the TEP's were negative with respect to the dilute medium, suggests that under the experimental circumstances the integumental barrier is preferentially cation conductive. The TEP's of the respiratory filaments were slightly more positive and those of the transport filaments slightly more negative than the diffusion potential for Na (−19 mV) calculated from the measured concentration difference. Cation selectivity is consistent with the data from other gill potential studies (*Austropotamobius = Astacus pallipes*, Croghan *et al.*, 1965; *Callinectes*, Mantel, 1967) and a study on the isolated gill cuticle of *Carcinus* (Lignon, 1987). Only a study by Avenet and Lignon (1985) presented data showing anion selectivity in the isolated cuticle from the gill lamina (plate) of *Astacus leptodactylus*. Whether the TEP's arise from diffusion potentials or from electrogenic transport is unknown, however, the contribution of transport-generated potentials is generally small in gills in the presence (Siebers *et al.*, 1985) or in the absence of concentration gradients (Siebers *et al.*, 1985; Drews and Graszynski, 1987). Avenet and Lignon (1985) and Lignon (1987) suggested that the ion selectivity of the integumental barrier resided in the epicuticle. Such cation selectivity of the epicuticle of the gill of *Procambarus* would be consistent with the location of the silver precipitate within the exocuticle. Presumably, the divalent silver cations could easily cross the outer cuticular barrier to precipitate with higher internal concentrations of chloride or, more likely, bicarbonate. If the observed TEP's are the result of diffusion potentials, the differences in TEP's between the respiratory and transport filaments would suggest either different ion permeabilities or different local ion concentrations within the two types of filaments.

The circulation of hemolymph within the gill filament has been described by Bock (1925), Fisher (1972), and Burggren *et al.* (1974). They describe hemolymph as flowing toward the tip of the filament in the afferent channel and down the filament toward the gill stalk in the efferent channel. Hemolymph may also be shunted from the afferent to the efferent channels via the lateral lacunae. The thick septum of connective tissue in respiratory filaments may act as a permeability barrier to counter-current gas exchange between the deoxygenated afferent hemolymph and the oxygenated efferent hemolymph, because this type of exchange would result in deoxygenated blood being returned to the body. The thin septum of the transporting filaments, on the other hand, may promote counter-current diffusion of ions from the afferent to the efferent channel, preventing further diffusive ion loss from the lacunae.

The observations in the present study indicate that there is a precise partitioning of structural and functional epithelium types within the gills of *Procambarus clarkii*, a thin squamous epithelium functioning in respiration and

a thick, mitochondria-rich epithelium functioning in ion transport. It is important to remember, however, that the integument consists not only of the underlying epithelium, but also of the overlying cuticle. Because this cuticle must periodically be shed to permit growth, the question arises as to whether the specialized functions of the filaments are disrupted during the period surrounding ecdysis. During premolt the hypodermis is normally engaged in cuticular synthesis, and prior to ecdysis the preexuvial cuticle exists as an additional barrier to the movement of substances. A more complete understanding of gill function must await examination of gills not only during intermolt, but also during the molt.

Literature Cited

Avenet, P., and J. M. Lignon. 1985. Ionic permeabilities of the gill lamina of the crayfish, *Astacus leptodactylus* (E). *J. Physiol.* **363:** 377–401.

Bielawski, J. 1971. Ultrastructure and ion transport in gill epithelium of the crayfish, *Astacus leptodactylus* Esch. *Protoplasma* **73:** 177–190.

Bock, F. 1925. Die Respirationsorgane von *Potamobius astacus* Leach. (*Astacus fluviatilis* Fabr.) Ein Beitrag zur Morphologie der Decapoden. *Z. Wiss. Zool.* **124:** 51–117.

Bryan, G. W. 1959. Sodium regulation in the crayfish *Astacus fluviatilis*. I. The normal animal. *J. Exp. Biol.* **37:** 83–99.

Bubel, A., and M. B. Jones. 1974. Fine structure of the gills of *Jaera nordmanni* (Rathke) [Crustacea, Isopoda]. *J. Mar. Biol. Assoc. U.K.* **54:** 737–743.

Burggren, W. W., B. R. McMahon, and J. W. Costerton. 1974. Branchial water- and blood-flow patterns and the structure of the gill of the crayfish *Procambarus clarkii*. *Can. J. Zool.* **52:** 1511–1518.

Cioffi, M. 1984. Comparative ultrastructure of arthropod transporting epithelia. *Am. Zool.* **24:** 139–156.

Compère, P., S. Wanson, A. Péqueux, R. Gilles, and G. Goffinet. 1989. Ultrastructural changes in the gill epithelium of the green crab *Carcinus maenas* in relation to the external salinity. *Tissue Cell* **21:** 299–318.

Copeland, D. E. 1963. Possible osmoregulatory cells in crab gills. *J. Cell Biol.* **19:** 16A.

Copeland, D. E. 1967. A study of salt secreting cells in the brine shrimp (*Artemia salina*). *Protoplasma* **63:** 363–384.

Copeland, D. E. 1968. Fine structure of salt and water uptake in the land-crab, *Gecarcinus lateralis*. *Am. Zool.* **8:** 417–432.

Copeland, D. E., and A. T. Fitzjarrell. 1968. The salt absorbing cells in the gills of the blue crab (*Callinectes sapidus* Rathbun) with notes on modified mitochondria. *Z. Zellforsch.* **92:** 1–22.

Croghan, P. C., R. A. Curra, and A. P. M. Lockwood. 1965. The electrical potential difference across the isolated gills of the crayfish *Austropotamobius pallipes* (Lereboullet). *J. Exp. Biol.* **42:** 463–474.

Diamond, J. M., and W. H. Bossert. 1968. Functional consequences of ultrastructural geometry in "backwards" fluid-transporting epithelia. *J. Cell Biol.* **37:** 694–702.

Doughtie, D. G. and K. R. Rao. 1981. The syncytial nature and phagocytic activity of the branchial podocytes in the grass shrimp, *Palaemonetes pugio*. *Tissue Cell* **13:** 93–104.

Drach, P., and C. Tchernigovtzeff. 1967. Sur la méthode de détermination des stades d'intermue et son application générale aux crustacés. *Vie Milieu* **18:** 595–610.

Drews, G., and K. Graszynski. 1987. The transepithelial potential difference in the gills of the fiddler crab, *Uca tangeri*: influence of some inhibitors. *J. Comp. Physiol.* **157B:** 345–353.

Dunel-Erb, S., J.-C. Massabuau, and P. C. Laurent. 1982. Organisation fonctionelle de la branchie d'ecrevisse. *C. R. Seances Soc. Biol.* **176:** 248–258.

Ehrenfeld, J. 1974. Aspects of ionic transport mechanisms in crayfish *Astacus leptodactylus*. *J. Exp. Biol.* **61:** 57–70.

Ernst, S. A. 1972. Transport adenosine triphosphatase cytochemistry. II. Cytochemical localization of ouabain-sensitive, potassium-dependent phosphatase activity in the secretory epithelium of the avian salt gland. *J. Histochem. Cytochem.* **20:** 23–28.

Ernst, S. A., C. V. Riddle, and K. J. Karnaky, Jr. 1981. Relationship between localization of Na^+-K^+-ATPase, cellular fine structure, and reabsorptive and secretory electrolyte transport. Pp. 355–385 in *Current Topics in Membranes and Transport*, V. 30, F. Bronner and A. Kleinzeller, eds. Academic Press, New York.

Finol, H. J., and P. C. Croghan. 1983. Ultrastructure of the branchial epithelium of an amphibious brackish-water crab. *Tissue Cell* **15:** 63–75.

Fisher, J. M. 1972. Fine-structural observations on the gill filaments of the freshwater crayfish, *Astacus pallipes* Lereboullet. *Tissue Cell* **4:** 287–299.

Foster, C. A., and H. D. Howse. 1978. A morphological study on gills of the brown shrimp, *Penaeus aztecus*. *Tissue Cell* **10:** 77–92.

Holliday, C. W. 1985. Salinity-induced changes in gill Na, K-ATPase activity in the mud fiddler crab, *Uca pugnax*. *J. Exp. Zool.* **233:** 199–208.

Horiuchi, S. 1977. Characterization of gill Na, K-ATPase in the freshwater crayfish, *Procambarus clarkii* (Girard). *Comp. Biochem. Physiol.* **56B:** 135–138.

Huxley, T. H. 1896. *The Crayfish—An Introduction to the Study of Zoology*. The Internat. Scientific Series. Paul, Trench and Trubner. London.

Johnson, P. T. 1980. *The Histology of the Blue Crab, Callinectes sapidus. A Model for the Decapoda*. Praeger. New York. Pp. 34–40.

Ishii, K., K. Ishii, J.-C. Massabuau, and P. Dejours. 1989. Oxygen-sensitive chemoreceptors in the branchio-cardiac veins of the crayfish, *Astacus leptodactylus*. *Resp. Physiol.* **78:** 73–81.

Kikuchi, S. 1983. The fine structure of the gill epithelium of a freshwater flea, *Daphnia magna* (Crustacea: Phyllopoda) and changes associated with acclimation to various salinities. I. Normal fine structure. *Cell Tissue Res.* **229:** 253–268.

Lignon, J. M. 1987. Ionic permeabilities of the isolated gill cuticle of the shore crab *Carcinus maenas*. *J. Exp. Biol.* **131:** 159–174.

Maluf, N. S. R. 1940. The uptake of inorganic electrolytes by the crayfish. *J. Gen. Physiol.* **24:** 151–167.

Mantel, L. H. 1967. Asymmetry potentials, metabolism and sodium fluxes in gills of the blue crab, *Callinectes sapidus*. *Comp. Biochem. Physiol.* **20:** 743–753.

Mantel, L. H., and J. Landesman. 1977. Osmotic regulation and Na-K-activated ATPase in the green crab, *Carcinus maenas* and the spider crab *Libinia emarginata*. *Biol. Bull.* **153:** 437–438.

Massabuau, J.-C., B. Elancher, and P. Dejours. 1980. Ventilatory reflex response to hypoxia in the crayfish, *Astacus pallipes*. *J. Comp. Physiol.* **140:** 193–198.

Milne, D. J., and R. A. Ellis. 1973. The effect of salinity acclimation on the ultrastructure of the gills of *Gammarus oceanicus* (Segerstrale, 1947) (Crustacea: Amphipoda). *Z. Zellforsch.* **139:** 311–318.

Morse, H. C., P. J. Harris, and E. J. Dornfeld. 1970. *Pacifastacus leniusculus*: fine structure of the arthrobranch with reference to active ion uptake. *Trans. Am. Micr. Soc.* **89:** 12–27.

Neufeld, G. J., C. W. Holliday, and J. B. Pritchard. 1980. Salinity adaptation of gill Na, K-ATPase in the blue crab, *Callinectes sapidus*. *J. Exp. Zool.* **211:** 215–224.

Péqueux, A., and R. Gilles. 1978. Osmoregulation of the euryhaline Chinese crab *Eriocheir sinensis*. Ionic transports across isolated perfused gills as related to the salinity of the environment. Pp. 105–111 in *Proc. 12th EMBS, Stirling, Scotland*. Pergamon Press, Oxford.

Péqueux, A., and R. Gilles. 1981. Na^+ fluxes across isolated perfused gills of the Chinese crab *Eriocheir sinensis*. *J. Exp. Biol.* **92:** 173–186.

Péqueux, A., and R. Gilles. 1988. The transepithelial potential difference of isolated perfused gills of the Chinese crab *Eriocheir sinensis* acclimated to fresh water. *Comp. Biochem. Physiol.* **89A:** 163–172.

Peterson, G. L. 1977. A simplification of the protein assay method of Lowry *et al.* which is more generally applicable. *Anal. Biochem.* **83:** 346–356.

Reynolds, E. S. 1963. The use of lead citrate at high pH as an electron opaque stain in electron microscopy. *J. Cell Biol.* **17:** 208–212.

Roer, R. D., and M. G. Shelton. 1982. The effects of hydrostatic pressure on sodium transport in the crayfish, *Procambarus clarkii*. *Comp. Biochem. Physiol.* **71A:** 271–276.

Shaw, J. 1960a. The absorption of sodium ions by the crayfish, *Astacus pallipes* Lereboullet. II. The effect of the external anion. *J. Exp. Biol.* **37:** 534–547.

Shaw, J. 1960b. The absorption of sodium ions by the crayfish *Astacus pallipes* Lereboullet. III. The effect of other cations in the external solution. *J. Exp. Biol.* **37:** 548–556.

Siebers, D., A. Winkler, C. Lucu, G. Thedens and D. Weichart. 1985. Na-K-ATPase generates an active transport potential in the gills of the hyperregulating shore crab *Carcinus maenas*. *Mar. Biol.* **87:** 185–192.

Spurr, A. R. 1969. A low-viscosity epoxy resin embedding medium for electron microscopy. *J. Ultrastruct. Res.* **26:** 31–43.

Stevenson, J. R. 1972. Changing activities of the crustacean epidermis during the molt cycle. *Am. Zool.* **12:** 373–380.

Strangeways-Dixon, J., and D. S. Smith. 1970. The fine structure of the gill "podocytes" in *Panulirus argus* (Crustacea). *Tissue Cell* **2:** 611–624.

Taylor, H. H., and P. Greenaway. 1979. The structure of the gills and lungs of the arid-zone crab, *Holthuisana* (*Austrothelphusa*) *transversa* (Brachyura: Sundathelphusidae) including observation on arterial vessels within the gills. *J. Zool.* **189:** 359–384.

Towle, D. W. 1984. Membrane-bound ATPases in arthropod ion-transporting tissues. *Am. Zool.* **24:** 177–185.

Towle, D. W. 1985. Localization of $Na^+ + K^+$-ATPase in basolateral membranes of crab (*Carcinus maenas*) gill epithelium. *Bull. MDIBL* **25:** 80–83.

Towle, D. W., and W. T. Kays. 1986. Basolateral localization of $Na^+ + K^+$-ATPase in gill epithelium of two osmoregulating crabs, *Callinectes sapidus* and *Carcinus maenas*. *J. Exp. Zool.* **239:** 311–318.

Wanson, S. A., A. J. R. Péqueux, and R. D. Roer. 1984. Na^+ regulation and the $(Na^+ + K^+)$ATPase activity in the euryhaline fiddler crab *Uca minax* (Le Conte). *Comp. Biochem. Physiol.* **79A:** 673–678.

Wheatly, M. G., and R. P. Henry. 1987. Branchial and antennal gland Na^+/K^+-dependent ATPase and carbonic anhydrase activity during salinity acclimation of the euryhaline crayfish *Pacifastacus leniusculus*. *J. Exp. Biol.* **133:** 73–86.

Wheeler, A. P. 1975. Oyster mantle carbonic anhydrase: evidence for plasma membrane bound activity and for a role in bicarbonate transport. Ph.D. Dissertation, Duke University. Durham, North Carolina.

Wright, K. A. 1964. The fine structure of the nephrocyte of the gills of two marine decapods. *J. Ultrastructure Res.* **10:** 1–13.